



HAL
open science

Mechanical vulnerability of beech (*Fagus sylvatica* L.) poles after thinning: securing stem or roots is risk dependent

Jana Dlouha, Pauline Défossez, Joel Hans DONGMO KEUMO JIAZET, François Ningre, Meriem Fournier, Thiéry Constant

► To cite this version:

Jana Dlouha, Pauline Défossez, Joel Hans DONGMO KEUMO JIAZET, François Ningre, Meriem Fournier, et al.. Mechanical vulnerability of beech (*Fagus sylvatica* L.) poles after thinning: securing stem or roots is risk dependent. 2024. hal-04233557

HAL Id: hal-04233557

<https://hal.science/hal-04233557v1>

Preprint submitted on 9 Oct 2023

HAL is a multi-disciplinary open access archive for the deposit and dissemination of scientific research documents, whether they are published or not. The documents may come from teaching and research institutions in France or abroad, or from public or private research centers.

L'archive ouverte pluridisciplinaire **HAL**, est destinée au dépôt et à la diffusion de documents scientifiques de niveau recherche, publiés ou non, émanant des établissements d'enseignement et de recherche français ou étrangers, des laboratoires publics ou privés.

1 **Mechanical vulnerability of beech (*Fagus sylvatica* L.) poles after thinning: securing stem or**
2 **roots is risk dependent**

3

4 Jana Dlouhá^{a,+}, Pauline Défossez^b, Joel H.D.K. Jiazet^a, François Ningre^a, Meriem Fournier^a, Thiéry
5 Constant^a

6 ^a Université de Lorraine, AgroParisTech, INRAE, UMR Silva, 54000 Nancy, France

7 ^b INRAE, Bordeaux Sciences Agro, ISPA, F-33140 Villenave d'Ornon, France

8 + Corresponding author.

9 *E-mail address:* jana.dlouha@inrae.fr (J. Dlouhá)

10

11 **Keywords:** mechanical acclimation – anchorage – thinning – guying – stem and root growth – beech

12

13 **Highlights**

- 14 • No directional anisotropy in the root anchorage was detected.
15 • Thinning surprisingly decreases the root-soil mechanical performances for a given tree
16 biomass when compared to control trees.
17 • The biomass allocation is adapted to the reinforcement of the mechanical weakest points, in
18 the case of beech poles, the stem and not the root system.
19

19

20 **Abstract**

21 In this study, we analysed how the tree growth in stem and roots reacts to thinning, focusing on
22 consequences on mechanical stability of the root-soil plate quantified by field mechanical bending
23 tests. In order to disentangle the role of the biomechanical control of growth (thigmomorphogenesis)
24 from other factors, half of the studied trees were guyed to remove mechanical stimulation of living
25 cells. Surprisingly, our results show a decrease in the root-soil plate mechanical performances for a
26 given tree biomass after thinning. This decrease was however explained by boosted biomass allocation
27 to the stem at the expense of the root system. Further, relationship between the initial stiffness and the
28 strength (overturning moment) of the root-soil plate was modified by thinning. It is suggested that at
29 this development stage (poles), as stem break is the weakest point of tree resistance to wind loads, the
30 biomechanical control of growth strengthen preferentially the stem and not the anchorage. Further
31 developments should study the diversity of behaviours between development stages (as older beeches
32 are prone to throw) and between species for a unified theory on the role of the thigmomorphogenetic
33 syndrome in tree resistance to wind risk, with synergies and trade-offs with other processes and
34 functions.

35

36 **1. Introduction**

37 Release of competition by thinning promotes the growth of retained trees taking advantage of increased
38 light and nutrients availability. However, retained trees experience also higher mechanical strains due

39 to higher penetration of the wind into the canopy and increased sway displacements due to the loss of
40 the stabilizing effect of collisions between adjacent trees (Rudnicki et al., 2008; Webb et al., 2013). It
41 is well known that forest stands are much more at risk of wind hazards after a thinning (Albrecht et al.,
42 2012; Cremer et al., 1982; Valinger and Fridman, 2011), in particular in the case of not recurrent and
43 intensive thinning (Albrecht et al., 2015). For example Wallentin and Nilsson (2014) followed wind
44 induced damage in recently thinned stands and observed a near-linear relationship between thinning
45 intensity and damage with 7, 42 and 74% of standing basal area damage in the control, normally and
46 heavily thinned plots, respectively (8, 53 and 89% thinning intensity). This initial increase in the
47 mechanical vulnerability is then followed by acclimation processes leading to an increase of wind
48 firmness however the transition is still poorly understood.

49 The period of acclimation after thinning lasts several years and is characterised by preferential biomass
50 allocation to the radial growth in the lower part of the stem and in structural roots and reduction of the
51 height growth (Dongmo Keumo Jiazet et al., 2022; Mitchell, 2000; Ruel et al., 2003; Vincent et al.,
52 2009). It has been recognized that allocation of the biomass to mechanically stimulated tissues is a
53 result of thigmomorphogenetic syndrome aiming to ensure mechanical stability of trees during their
54 life (Mouliia et al., 2015; Telewski, 2006). Root growth reaction seems to be strongly affected by
55 mechanical strains. Nicoll and Dunn (2000) reported few significant correlations between wind speed
56 and tree ring chronologies of stem growth, but many positive correlations with the tree ring
57 chronologies of root growth. Further, growth increase is often immediate in roots followed by one or
58 more years delayed growth reaction in the stem (Kneeshaw et al., 2002; Urban et al., 1994; Vincent et
59 al., 2009) however sometimes both compartments respond with a 1-yr delay (Nicoll et al., 2019) or
60 with no delay at all (Defosse et al., 2022).

61 Couple of authors tried to quantify the role of mechanical strains on the tree growth in a forestry context
62 coupling guying of trees with a thinning experiment, looking at the thigmomorphogenetic effect in two
63 resource availability conditions. Defosse et al. (2022) focused on the 16 years old *P. pinaster* stem
64 growth during three years after thinning and guying (a treatment that removes strains so mechanical
65 stimulations in growing stem tissues). They obtained similar magnitude but opposite effects of guying
66 and thinning on the stem growth without an interaction between both factors. Nicoll et al. (2019)
67 reported inhibitory impact of guying on the stem and root radial growth in thinned trees in a young
68 spruce stand. Constant et al. (2018) reported that in dense beech pole stand, the mean stem growth rate
69 at DBH of unthinned trees free to sway was multiplied by a factor 0.5 for unthinned and guyed trees,
70 by 1.2 for thinned and guyed trees, and by 2.0 for thinned trees free to sway. Similar growth response
71 was also observed in roots of beech poles (Dongmo Keumo Jiazet et al., 2022), only for thinned and
72 guyed trees the ratio yielded 1.4 instead of 1.2. Mechanoperception seems therefore to play a major
73 role in the acclimation process of both, tree stem as well as structural roots.

74 As a result of mechanical acclimation, root systems of forest trees are often markedly asymmetric.
75 Roots on the leeward side of the tree in relation to the prevailing wind direction show higher diameter
76 growth and stronger taper than roots in other directions (Coutts et al., 2000). Specific cross-sectional
77 shapes similar to T-beams are developed on the lee-ward side of the tree (Nicoll and Ray, 1996). Nicoll
78 and Ray (1996) also reported that allocation to structural roots on the leeward side was strongly
79 correlated with maximum wind speeds and this allocation appeared to be at the expense of roots further
80 from the tree that would have had less of a structural role. Development of windward roots was
81 correlated well with maximum gusts in the corresponding years. We can hypothesize that considering
82 asymmetry of the tree growth, mechanical properties of the root-soil system may be also dependent on
83 the prevailing wind direction.

84 Assessing the anchorage strength change with the tree size is not as simple as for stem resistance which
85 is a function of the tree diameter elevated at power (Peltola, 2006). The root-soil plate is a composite
86 structure and therefore many parameters such as the soil type and its interaction with the root system
87 as well as the root system architecture and the root mechanical properties will contribute to determine
88 the overall anchorage capacity of a tree and mechanical modelling provides clues to understand the
89 role of each factor (Dupuy et al., 2007; Yang et al., 2018). In addition to these in silico approaches,
90 field experiments have been implemented. They impose a bending force (as wind forces are bending
91 forces) and measure the critical overturning moment which causes the failure (Gardiner et al., 2008).
92 This critical force is obviously size-dependant (the bigger the stronger): growth increases the anchorage
93 resistance against wind. However, because of the complexity of strength mechanisms in the root-soil
94 plate, the effect of increased growth is not so clear. Experimental field studies observed that the
95 overturning moment is globally a linear function of the stem biomass or another easy-to-measure
96 variable) (Lundstrom et al., 2007) and then the anchorage strength is characterized by the regression
97 slope i.e. the critical force for a given stem biomass, which is the parameter used in the wind risk
98 evaluation models to characterize the anchorage strength, removing the first order size effect (Gardiner
99 et al., 2000). Achim et al. (2005b) reported overturning moment in a balsam fir stands thinned 9 and
100 14 years earlier and did not observe any increase in anchorage strength. In contrast, other studies
101 reported higher anchorage strength in windy stands (Nicoll et al., 2008) or at the forest edge (Cucchi
102 et al., 2004) or in widely spaced plantations (Hale et al., 2012). The latter observations were interpreted
103 as a result of acclimation process to mechanical strains induced by wind. However, no study so far
104 reported thigmomorphogenetic effect on the tree anchorage capacity directly.

105 Existing reports dealing with the tree growth and anchorage response after thinning and/or guying in
106 the forest context focused exclusively on conifers. While growth responses are rather well documented,
107 little is known about the acclimation of the root anchorage strength. This study examines the growth
108 and anchorage capacity of beech poles after thinning and/or guying. Following hypothesis will be tested
109 in this manuscript:

110 H1: beech poles anchorage capacity and growth reaction after treatment will be stronger in the direction
111 of prevailing winds.

112 H2: preventing the perception of mechanical strains by guying will reduce the root anchorage while
113 increase in the mechanical strains due to thinning will increase the root anchorage. The increase should
114 be higher than just the size effect, i.e. the increase of strength proportional to biomass growth.

115 H3: guying will restrict the biomass allocation to mechanically stimulated parts of the tree.

116

117 **2. Materials and Methods**

118 *2.1. Stand site and experimental design*

119

120 The experimental site is located within the Haye Forest near Nancy, France (48°40'14.5"N;
121 6°05'10.3"E). Stand conditions are described in Bonnesoeur et al. (2016). The stand is a pure even-
122 aged *Fagus sylvatica* L. stand issued from natural regeneration with the Reineke's density index of
123 0.87 and no previous thinning. Experimental plot area is around 2 ha. At the end of 2014, poles were
124 c. 30 years old with an average height of 13.3m and an average diameter of 12.8cm. Four groups each
125 consisting of ten dominant trees were selected for the study. During the winter 2014/2015 two groups
126 were thinned removing neighbouring trees within a 4-meter radius circle centred on each target tree.

127 Such treatment corresponds to a very strong thinning intensity. Then, half of trees (ten thinned and ten
 128 unthinned) were guyed just below their living crown. Four treatments were therefore applied:
 129 unthinned trees free to sway (uTF), unthinned and guyed trees (uTG), thinned trees free to sway (TF)
 130 and thinned and guyed trees (TG). Trees from each group were paired according to morphologic
 131 criteria. Details about selection criteria and treatments application are given in (Dongmo Keumo Jiazet
 132 et al., 2022). The site climate is a degraded oceanic type with continental influence. Rainfall is heavy
 133 and well distributed over the year. Over the 4 years of the study, the mean annual rainfall was 700 mm
 134 and the average wind speed during the 4-year period was 3 m/s. Dominant winds came mainly from
 135 the South West quadrant.

136

137 2.2. Estimation of the tree biomass and mechanical properties of the tree stem and root-soil plate

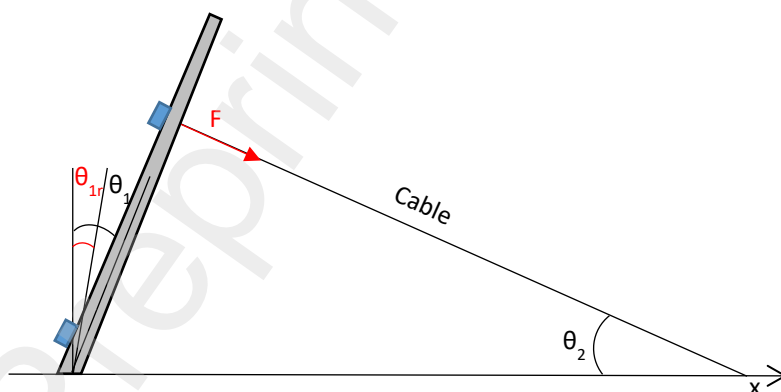
138

139 All forty beech poles were submitted to pulling tests starting from mid-March 2019 to end of April
 140 2019. The pulling set-up was based on Nicoll et al. (2006) and is displayed in Figure 1. Prior to the
 141 pulling test, the tree stem was cut at 3 m height to eliminate the contribution of the crown load (Coutts,
 142 1986). Trees were loaded using an electric winch (Winchmax, UK, maximal strength capacity 80 kN).
 143 The force applied to each sample tree was measured by a load cell (T20, AEP, Italy, maximum load
 144 100 kN). The height of the cable attachment was low enough on the stem to induce anchorage failure
 145 without stem breakage. The latter varied from tree to tree, ranging from 1.6 m to 2.3 m. The angle of
 146 the cable θ_2 was measured when the pulling cable was stretched with a portable inclinometer. Two
 147 inclinometers (IS2BP090-I-CL; GEMAC, France) were tied to the tree to measure the root-soil system
 148 rotation θ_{1r} (at the stem base) and the total tree inclination θ_1 (close to the cable attachment point). Data
 149 from the load cell and inclinometers were recorded by a logger at a sampling rate of 20 Hz (CR1000X;
 150 Campbell Scientific Ltd., France) and uploaded to a laptop computer for processing.

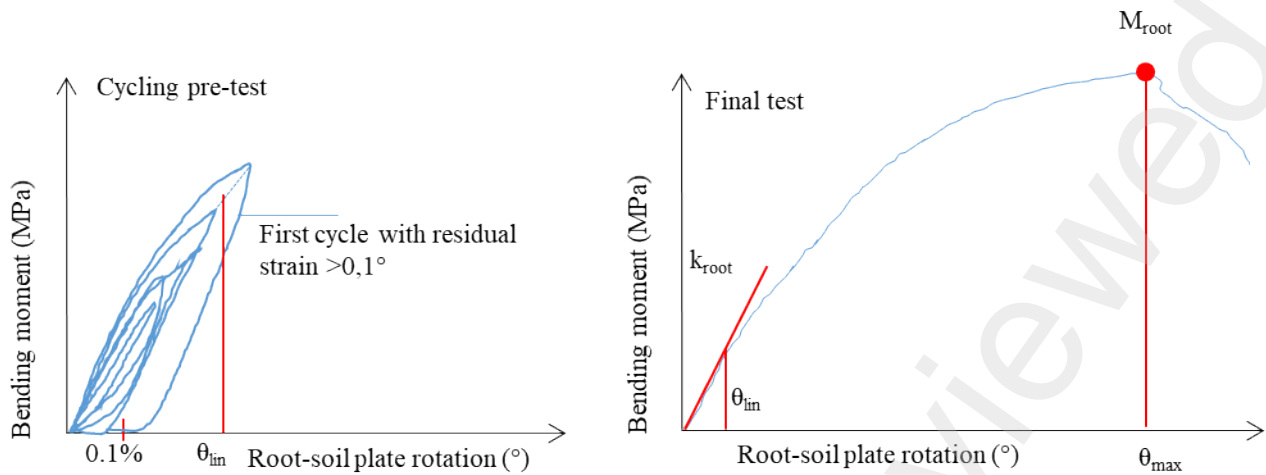
151 The turning moment M was calculated as follows:

$$152 \quad M = F_x L \cos \theta_1 + F_y L \sin \theta_1 \quad (1)$$

153 where θ_1 is the total rotation given by the deflection angle of the trunk at the cable attachment point
 154 with respect to the vertical, L is the height of the cable attachment point, $F_x = F \cos \theta_2$ and $F_y = F \sin \theta_2$
 155 are respectively the horizontal and vertical components of the force F measured in the cable, θ_2 the
 156 angle of the cable from the horizontal (Figure 1).



157 Figure 1: Set-up of the pulling test. θ_{1r} is the root-soil plate rotation, θ_1 is the trunk deflection angle and θ_2 is the cable
 158 inclination. F is the pulling force. Blue boxes represent location of inclinometers.



159

160 Figure 2: Estimation of mechanical performances of the root-soil plate from the experimental curve. θ_{lin} stands for the
 161 elastic strain limit, k_{root} stands for the initial root-soil plate elasticity and M_{root} stands for the overturning moment.
 162 Figures are not proportional, the pre-test figure is magnified in order to make the elastic limit visible.

163 The root-soil plate initial stiffness and the elastic limit were first assessed in the direction perpendicular
 164 to the prevailing wind direction (pre-test) followed by uprooting of the tree in the prevailing wind
 165 direction (final test). The pre-test consisted in a cycling procedure with a progressive increase of the
 166 applied load for every new cycle (see Fig. 2). Once the residual root-soil plate rotation after the tree
 167 unloading was higher than 0.1° , the test was stopped. Elastic limit (θ_{lin}) was therefore computed as an
 168 interpolated value between the last elastic load step and the first post-elastic load step. Trees were then
 169 pulled until the overturning thus obtaining the overturning moment (M_{root}) in the main wind direction.
 170 The root-soil plate initial stiffness (k_{root}) was computed as a slope between the turning moment and θ_{lin}
 171 in the elastic domain. To compute the root-soil plate initial stiffness in the prevailing wind direction,
 172 elasticity limit determined from the pre-test was used.

173 The stem resistance (M_{stem}) was computed as follows:

$$174 \quad M_{stem} = \frac{\pi * D^3 * MOR}{32},$$

175 where D is the tree diameter and MOR is the wood strength. As no effect of thinning and/or guying on
 176 the wood mechanical properties was detected (Dlouhá et al., 2023) the average value of the tensile
 177 strength was used for this computation *i.e.* 110 MPa. The tree biomass was weighted using a load cell
 178 as detailed in Dongmo Keumo Jiazet et al. (2022), it is therefore a direct measure and not estimation
 179 based on partial sampling and allometric relationships that might be affected by treatments underwent
 180 by studied trees.

181 2.3. Soil and root characterization

182 The study area is part of the larger area known as the Lorraine plateau ($6.1^\circ E$, $48.7^\circ N$). Three
 183 rectangular soil pits (1 m x 0.4 m) were manually dug in the stand down to the calcareous bedrock
 184 horizon. The soil is a rendosol where rooting is constrained by a stony layer with 70-90% of stones at
 185 34.3 ± 7.7 cm depth. Above this stony layer two clay-silt horizons may be distinguished with above and
 186 below 10 ± 1.2 cm depth, containing together all roots with diameter > 2 mm. Limestone bedrock is
 187 situated at 79.5 ± 14.8 cm. Once the root-soil plate extracted, the maximal rooting depth was measured

188 as well as the depth of two visible horizons. A soil sample of 0.25l (cylinder of 5 cm depth and 8 cm
189 of diameter) was taken in the middle of each horizon, placed in an aluminium box sealed with a plastic
190 foil for subsequent determination of gravimetric soil water content. Gravimetric soil water content was
191 determined by comparing fresh and dry weights (24 h at 105.0 °C) of the soil sample from each horizon.
192 Weighted gravimetric soil water content was then computed as a weighted mean taking into account
193 the depth of each soil horizon.

194 *2.4. Root growth ring measurements*

195 Extracted root systems were first cleaned in the forest with an air compressor before finer cleaning
196 using a high-pressure water in the laboratory. Four largest structural roots were cut at 0.25 m horizontal
197 distance from the stump centre. The selected roots were distributed around the tree to represent
198 different quadrants in respect to the wind direction, leeward quadrant (North-East) and windward
199 quadrant were designated by 1 and 2 respectively and quadrants perpendicular to the prevailing wind
200 direction were designated by 3 and 4. The biggest roots in each quadrant was selected and a 2-cm thick
201 cross-sectional root sample was scanned with an optical scanner at 600 dpi resolution and growth rings
202 were measured using Image-J software. The upper side of each root was marked and the root growth
203 ring widths were measured only in the maximal growth direction from the upper-side outer ring to the
204 biological centre of the root. For the sake of simplicity, we will not talk about average maximal root
205 growth ring indicator but about mean root growth ring. It happened that some quadrants could not be
206 sampled because roots were broken. Altogether, 122 root samples equally distributed among treatments
207 were measured. A stem disk was also collected at breast height to compare the growth response at the
208 stem and root level. The methodology to analyse stem and root samples is further detailed in Dongmo
209 Keumo Jiazet et al. (2022).

210 *2.5. Statistical analysis*

211 Statistical analyses were performed using R-software (R Core Team, 2020). We first used ANOVA on
212 lm model to check that there were no difference in the soil water content during pulling tests as well as
213 in the rooting depth of the tree groups. Afterwards, effects of thinning, guying and their interaction on
214 mean values of the root system properties summarized in Table 1 were assessed by linear mixed effects
215 models (nlme package) with pairing as a random effect. Different treatments were then compared using
216 emmeans package (joint_tests function). Effects of thinning, guying, and their interaction on
217 relationships between the root system mechanical properties and their predictor (stem biomass) or
218 between mechanical properties themselves, were assessed using gls models because their AIC were
219 systematically lower than for mixed effects models. Relationship between the root and the stem growth
220 increments before and after treatments were assessed using linear mixed effects models with tree
221 number as a random effect to take into account repeated measurements, introducing of pairing as a
222 random effect did not improve the model. We assessed the normality of the data distribution with Q-Q
223 plots, and homoscedasticity with standardized residuals against plotted fitted values and when
224 necessary with Levene tests (package car). Weighted regressions, in function of thinning, were used
225 for M_{root} against M_{stem} and M_{root} against k_{root} predictions.
226

227 **3. Results**

228 Table 1 shows that there was no difference in the soil water content between the four groups tested and
229 the rooting depth was also the same. Considering the effect of thinning, guying and their interaction on
230 the root-soil mechanical properties, results show that interaction factor (thinning x guying) was not

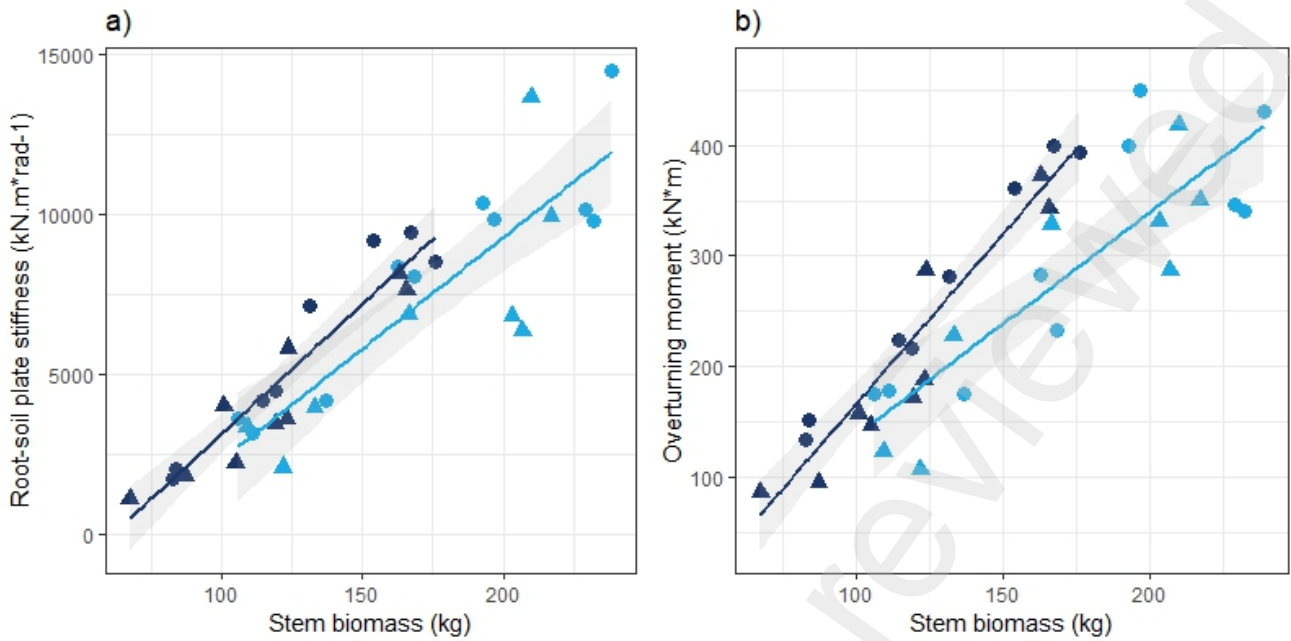
231 significant (Table 2) while thinning and guying effects were significant for all properties tested except
 232 for the strain at elastic limit and maximal strain, with very high significance especially for the stem
 233 resistance. Thinning strongly affected the stem biomass while guying effect was not detected.
 234 When comparing different treatments between them, the root-soil plate stiffness (k_{root}) and overturning
 235 moment (M_{root}) were significantly higher in thinned trees free to sway compared to unthinned and
 236 guyed trees. The stem resistance (M_{stem}) was significantly higher for thinned trees free to sway
 237 compared to all other treatments. Observed elastic limit of the root-soil plate rotation θ_{lin} does not differ
 238 with the treatment but was higher than the threshold typically used for the non-destructive evaluation
 239 of the tree failure (Brudi and Wassenaer, 2001; Detter et al., 2023) or identified in sub-alpine spruce
 240 (Jonsson et al., 2006) which was 0.25° and 0.5° respectively. However this limit was close to the elastic
 241 limit experienced by Eucalyptus trees in natural conditions (James et al., 2013) *i.e.* $0.88\text{-}0.9^\circ$.
 242

Treatment	Soil water content (%)	Root depth (cm)	k_{root} (kN.m/rad)	θ_{lin} ($^\circ$)	M_{root} (kN.m)	M_{stem} (kN.m)	θ_{max} ($^\circ$)	Stem biomass
TF	26.6 (2.2)	49.0 (2.5)	8196 ^a (1133)	1.0 (0.1)	301 ^a (34)	84.7 ^a (9.8)	10.9 (1.2)	177.4 ^a (15.5)
TG	25.9 (1.1)	42.7 (2.7)	6475 ^{ab} (1183)	0.9 (0.1)	274 ^{ab} (35)	58.3 ^b (7.3)	9.6 (1.3)	170.9 ^a (15.6)
uTF	29.2 (1.0)	41.6 (3.5)	5838 ^{ab} (1108)	1.2 (0.1)	270 ^{ab} (37)	54.9 ^b (6.9)	10.9 (1.0)	128.4 ^b (12.6)
uTG	26.1 (1.1)	46.9 (5.1)	4203 ^b (835)	1.1 (0.1)	205 ^b (35)	42.1 ^b (5.7)	10.7 (1.2)	117.2 ^b (10.8)

243
 244 Table 1: Mean values of the soil humidity, the rooting depth and the mechanical characteristics of the tree root and stem
 245 resistance for each treatment. Values in brackets stand for standard error. k_{root} is the root-soil rotation stiffness, M_{root} is the
 246 overturning moment, θ_{lin} is the strain at elastic limit, θ_{max} is the strain and M_{stem} is the stem resistance.
 247

	Thinning	Guying	Thinning x Guying
k_{root}	0.0029	0.0184	0.86
θ_{lin}	0.0532	0.4773	0.94
M_{root}	0.047	0.0107	0.18
θ_{max}	0.3028	0.1834	0.37
M_{stem}	0.0002	0.0001	0.39
Stem biomass	<0.001	0.0620	0.56

248
 249 Table 2: p-values of the main effects and their interaction (guying and thinning) of linear mixed effect models. k_{root} is the
 250 root-soil rotation stiffness, M_{root} is the overturning moment, θ_{lin} is the strain at elastic limit and M_{stem} is the stem resistance.
 251
 252

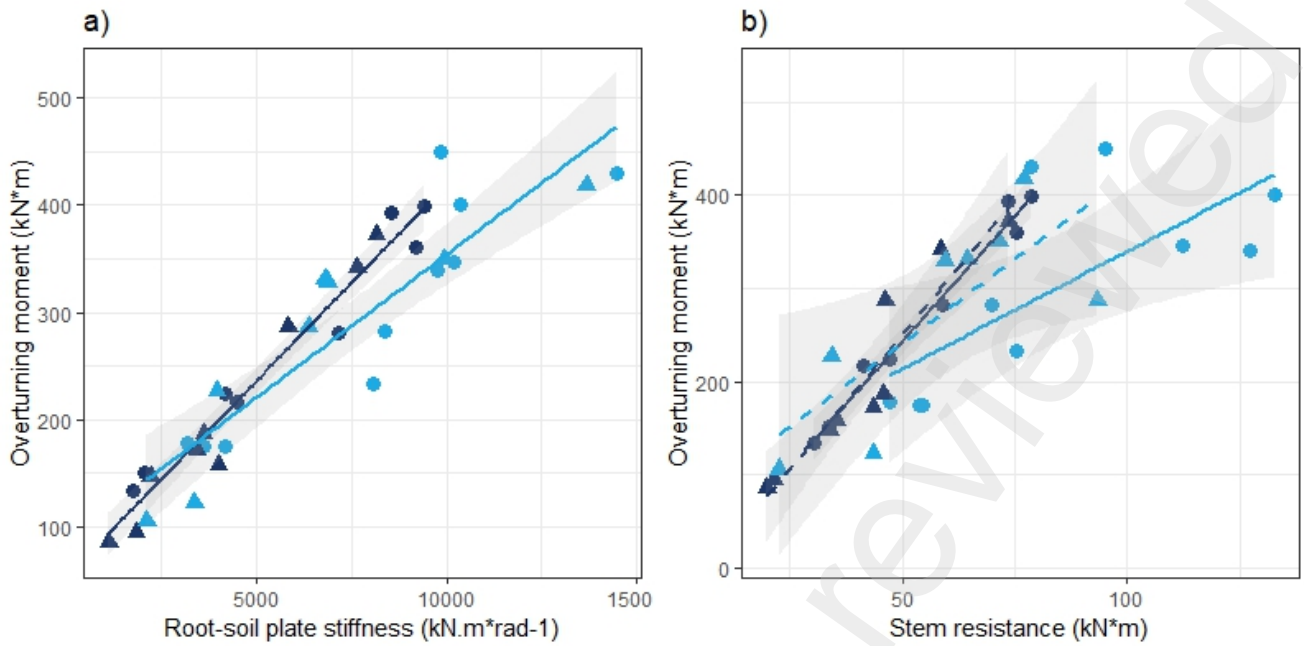


253
 254 Figure 3: a) Relationship between the root-soil plate stiffness and the stem biomass. b) Relationship between the overturning moment and stem biomass. Dark blue regression lines and points represent unthinned trees. Light blue regression lines and points represent thinned trees. Triangles stand for guyed trees and circles for trees free to sway.
 255
 256

	Effects on intercept			Effects on slope		
	Thinning	Guying	Thinning x Guying	Thinning	Guying	Thinning x Guying
$k_{root} \sim \text{Stem biomass}$	0.04	0.09	0.95	0.48	0.70	0.64
$M_{root} \sim \text{Stem biomass}$	0.0003	0.18	0.95	0.04	0.58	0.77
$M_{root} \sim k_{root}$	0.03	0.52	0.80	0.015	0.32	0.30
$M_{root} \sim M_{stem}$	0.03	0.28	0.54	0.006	0.40	0.69

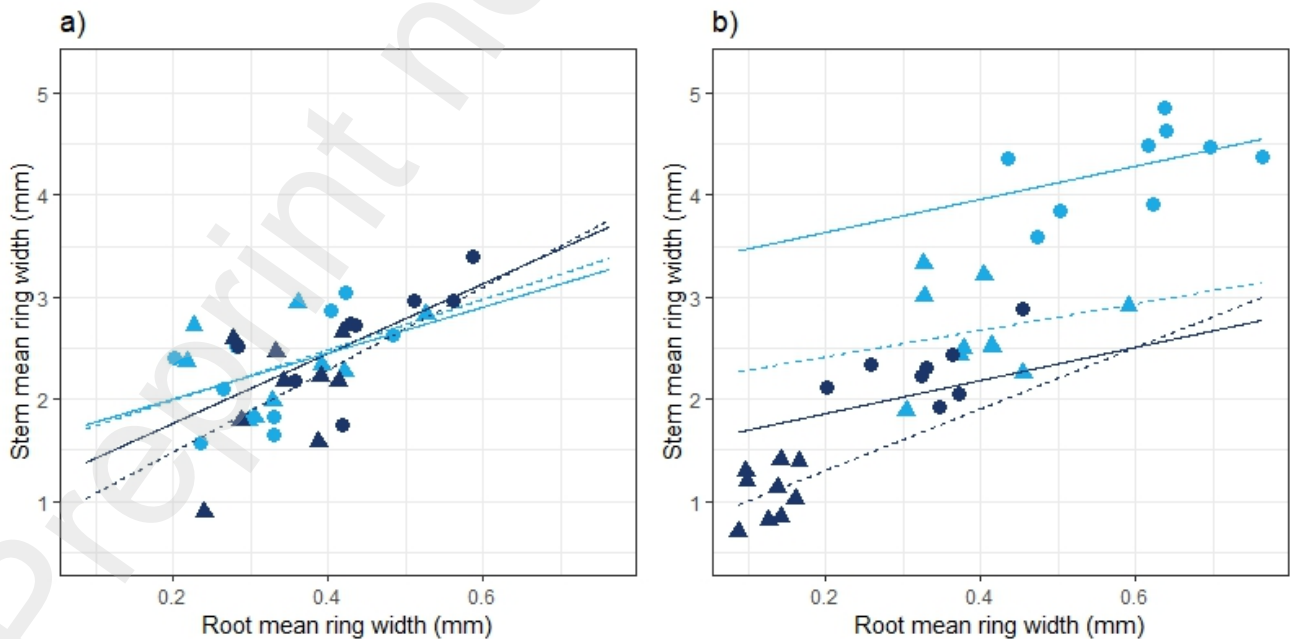
257
 258 Table 3: p-values (gls models) of main effects and their interaction on relationships between the root system mechanical
 259 properties and the stem biomass or between different root and stem mechanical properties.

260 Figure 3 shows the relationship between the root-soil plate stiffness and the overturning moment
 261 against the tree stem biomass. We can see that thinned trees display surprisingly lower root system
 262 anchorage properties for a given tree biomass compared to unthinned trees. In the root-soil plate
 263 stiffness case, the regression line for thinned trees is shifted downwards while for the overturning
 264 moment, thinning affects the intercept as well as the slope of the relationship against the stem biomass
 265 (see Table 3). For example a tree with 150kg stem biomass from the unthinned plot will achieve an
 266 overturning moment of 336kN*m/rad against 232kN*m for a 150kg tree from the thinned plot which
 267 is a decrease of 44.8%.



268
 269 Figure 4: a) Relationship between the overturning moment and the root-soil plate initial stiffness. b) Relationship between
 270 the overturning moment and the stem resistance. Dark blue lines and points represent unthinned trees. Light blue lines
 271 and points represent thinned trees. Triangles stand for guyed trees and circles for trees free to sway. Solid lines represent
 272 regression line for trees free to sway and dotted lines represent regression lines for guyed trees.

273 Figure 4a shows that after thinning, the slope of the regression line between the overturning moment and
 274 the root-soil plate elasticity is lower. Considering the balance between the overturning moment
 275 and the stem resistance (Figure 4b), we can clearly see that thinned trees free to sway (dark solid line)
 276 invest more in their stem resistance compared to the anchorage and this trend is reduced by guying
 277 (dotted line). When comparing selected contrasts, TF has lower slope than uTF and uTG (p-values
 278 0.036 and 0.017 respectively) while there is no statistical difference between TF and TG. The slope
 279 (estimate and standard error) of the regression is of 2.52 ± 0.85 for TF, 3.60 ± 1.26 for TG and 5.38 ± 0.55
 280 for uTF and 5.77 ± 0.58 for uTG.



281

282 Figure 5: Relationship between the stem mean ring width and the root mean ring width before (a) and after treatments (b).
 283 Each point represents the mean growth ring width over a four years period. Light blue regression lines and points represent
 284 thinned trees, dark blue regression lines and point represent unthinned trees. Triangles stand for guyed trees and circles for
 285 trees free to sway. Solid lines represent regression line for trees free to sway and dotted lines represent regression lines for
 286 guyed trees.
 287

Effect	p-value
(Intercept)	<.0001
Guying	<.0001
Thinning	<.0001
Period	0.0001
Root_ring	<.0001
Guying:Period	0.0043
Thinning x Period	0.0003
Guying x Root_ring	0.0130
Thinning x Root_ring	0.6446
Period x Root_ring	0.1070

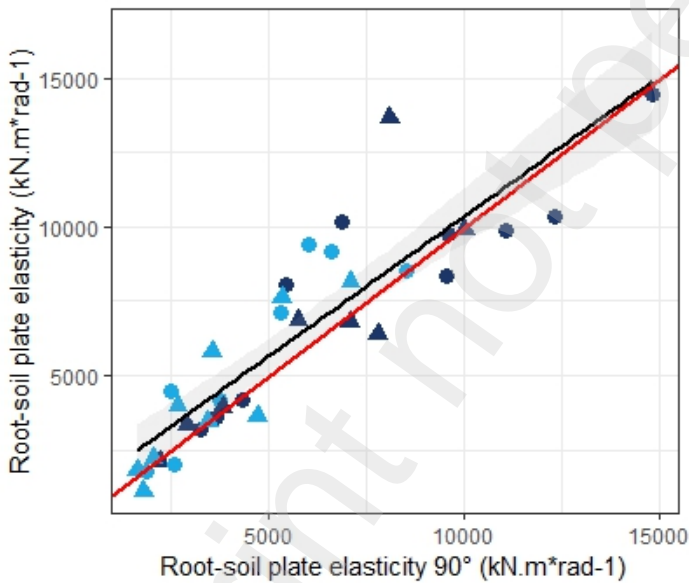
288
 289
 290 Table 4: p-values (linear mixed effects models) for main effects and their interaction on the relationship between the
 291 mean growth ring in the stem and in roots.
 292

293 After the analysis of the root and stem mechanical properties, we measured the biomass allocation
 294 between the tree compartments (stem and structural roots) before and after the treatments. We looked
 295 first at the mean root and stem growth ring over the period of four years. Fig. 5a shows that there is no
 296 significant difference between the four groups before treatments. Table 4 further shows that main
 297 effects (guying, thinning and period) are concentrated on the intercept which is confirmed in the Fig.
 298 5b where regression lines for each treatment are horizontally shifted. When comparing selected
 299 contrasts, TG and uTF trees do not show any change in the biomass allocation between the tree
 300 compartments before and after the treatments (p-values 0.61 and 1 respectively) while TF clearly
 301 allocate more biomass to the stem compared to structural roots after thinning (p-value 0.0019).
 302

Treatment	Direction	Before		After	
		Root growth (mm)	Standard error (mm)	Root growth (mm)	Standard error (mm)
uTF	1	0.53	0.04	0.38	0.03
uTF	2	0.39	0.04	0.30	0.03
uTF	3	0.45	0.03	0.33	0.02
uTF	4	0.42	0.04	0.31	0.03
uTG	1	0.34	0.03	0.12	0.01
uTG	2	0.35	0.03	0.12	0.01
uTG	3	0.34	0.05	0.18	0.03
uTG	4	0.41	0.04	0.17	0.02
TF	1	0.36	0.03	0.69	0.03
TF	2	0.31	0.03	0.53	0.04
TF	3	0.35	0.04	0.60	0.03
TF	4	0.31	0.03	0.54	0.03
TG	1	0.34	0.02	0.45	0.03
TG	2	0.30	0.03	0.35	0.03
TG	3	0.37	0.03	0.40	0.03
TG	4	0.34	0.04	0.33	0.02

303
304
305

Table 5: Mean values of the root ring width for a given treatment, time period and direction. Direction 1=NorthEast, leeward side, direction 2 = SouthWest, direction 3=SouthEast, direction 4=NorthWest.



306

307 Figure 6: Relationship between the root-soil plate stiffness in the direction of the main wind loading against the root-soil
308 plate stiffness in the direction perpendicular to the main wind loading. Red line represents the $y = x$ line. Light blue
309 regression lines and points represent thinned trees, dark blue regression lines and point represent unthinned trees.
310 Triangles stand for guyed trees and circles for trees free to sway.

311 We further looked at the directional allocation of the biomass in roots in function of the main wind
312 direction. Mean root ring and its standard error for a given treatment, period and direction is
313 summarized in Table 5. Results of statistical tests revealed no effect of the direction before treatments
314 ($p = 0.13$) while after treatments, direction was statistically significant ($p = 0.00$). Paired tests showed
315 that the direction 1 (leeward side) was significantly different from direction 2 and 4 (p -values 0.0002
316 and 0.0008 respectively) however no difference with direction 3 was detected which has no

317 biomechanical meaning (we would expect more allocation along the dominant wind axis *i.e.* direction
318 1&2). Further, the interaction term between the treatment and direction is not significant ($p=0.14$).
319 Figure 6 shows that there is no anisotropy in the root-soil plate initial stiffness with respect to the
320 pulling direction neither which is in agreement with the ring width results. When we looked at
321 confidence interval of the regression parameters, the slope is not significantly different from unity
322 ($p=0.49$) and the intercept not significantly different from zero ($p=0.096$).

323 4. Discussion

324 *4.1. No directional anisotropy was detected in the growth of structural roots and the initial root-soil* 325 *plate stiffness*

326 Root systems often exhibit anisotropic growth with more structural root mass on the leeward side than
327 the windward side of the tree relative to the prevailing wind direction (Nicoll and Ray, 1996). However
328 data about the directional dependence of mechanical performances of the root-soil plate are lacking. In
329 this study, we measured the initial stiffness of the root-soil plate in two directions: the prevailing wind
330 direction and perpendicular to it. No directional difference was observed in the initial stiffness of the
331 root-soil plate (Fig. 6) however the latter may reflect more the development of fine roots and coherence
332 of the root system with the neighbouring soil than the thickening of structural roots that is involved in
333 later phases of mechanical loading even if both parameters are in general well related (Jonsson et al.,
334 2006). We therefore looked also at the growth in structural roots in function of the direction of the wind
335 loading however again, no directional preference for biomass allocation was detected along the wind
336 direction axis. This result is in agreement with the fact that even if the wind loading at our site is
337 anisotropic with a defined prevailing wind direction, anisotropy of the mechanical strain perceived at
338 the periphery of the stem is much lower and likely not anisotropic enough to trigger anisotropic
339 distribution of the growth around the stem periphery (Dongmo Keumo Jiazet, 2022).

340 *4.2. Thinning surprisingly decreased the mechanical properties of the root-soil plate for a given tree* 341 *biomass*

342 It is widely accepted that thinning reduces the long-term risk of wind damage. However, immediately
343 after the thinning trees are on the contrary more prone to fail mechanically (Wallentin and Nilsson,
344 2014). This initial mechanical vulnerability after thinning is in general attributed to increased wind
345 penetration into the canopy and lack of neighbours, when the intrinsic resistance of trees is not yet
346 acclimated to new conditions. Thigmomorphogenetic syndrome expects increased biomass allocation
347 to the tree parts experiencing high strains, typically the bottom part of the stem and structural roots in
348 order to reduce the mechanical risk, increasing the mechanical strength of the anchorage during the
349 few years of the transition period after thinning. Indeed, a couple of studies report increase in the root
350 growth after thinning and that is hindered by guying (Dongmo Keumo Jiazet et al., 2022; Nicoll et al.,
351 2019). However the relation between the root growth and the change in root-soil plate mechanical
352 properties is not straightforward. Considering the root-soil plate mechanical properties, to our
353 knowledge only the effect of thinning was reported and no study exists on the root-soil plate mechanical
354 properties of guyed trees. Achim et al. (2005a) studied the effect of thinning on the overturning moment
355 of balsam fir 9 and 14 years after thinning and did not show any effect of thinning on the relationship
356 between the overturning moment and stem biomass. But 9 and a fortiori 14 years after the thinning, the
357 transition period might be over, thus only confirming the finding that different spacing does not affect
358 the overturning moment-stem biomass relationship as established by Nicoll et al. (2009) and confirmed
359 recently for example by Kamimura et al. (2017).

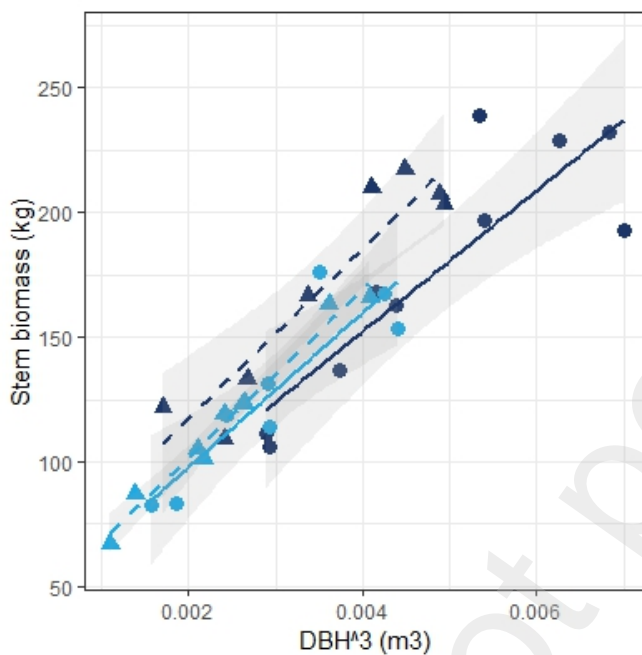
360 Surprisingly, our study shows lower mechanical properties of the root-soil plate for a given tree
361 biomass after thinning for the elastic part of the response as well as for the final overturning moment
362 (Fig. 3). Such finding might at the first sight contradict the capacity of the thigmomorphogenetic
363 syndrome to ensure the mechanical security of the tree. It was also found that the relationship between
364 the initial stiffness of the root-soil plate increased more than the overturning moment after the thinning
365 (Fig. 4). As mentioned by Yang et al. (2020), the elastic stiffness of the root-soil plate is crucial for the
366 mechanical stability of the tree due to the fatigue in roots system occurring during successive wind
367 gusts and therefore it should be reinforced in priority. Whereas removing the perception of the
368 mechanical signal have changed cambial growth in stems and roots (Dongmo Keumo Jiazet 2022), no
369 effects were detected on the scaling of mechanical properties of the root-soil plate with the stem
370 biomass. As the mechanical behaviour of the root-soil plate is not, on the contrary to the stem, mainly
371 influenced by the radial growth of one single beam, it will be interesting to study more accurately
372 changes of root architecture after thinning and trade-offs between several needs and constraints. Indeed,
373 the biomass of fine roots is known to significantly increase after thinning (López et al., 2003) and
374 change in the fine root biomass production is found to be more sensitive to thinning than in thicker
375 structural roots (Pang et al., 2022). It might be very interesting to check the proportions of fine roots
376 in further studies and study their role in mechanical properties. Then, for further ecological studies, we
377 suggest to study to which extent the initial stiffness of the root-soil plate might be used as a mechanical
378 but also hydraulic trait.

379 The main clue to enlighten the unexpected decrease of the root-soil plate mechanical properties with
380 thinning is given in Fig. 4b showing the relationship between the overturning moment and the stem
381 resistance. We can see that the slope of the regression is high in unthinned trees (5.38 for uTF, 5.77 for
382 uTG) and is reduced in TG (3.60) and in particular in TF trees (slope = 2.52). Forest managers know
383 that for this size of beech trees, the stem break represents the main mechanical risk and this is likely
384 the reason why the mechanical properties of the root system for a given tree biomass are not really
385 controlled by biomechanics and can be lower after the thinning. This finding is also in line with the
386 model prediction of windthrow probability that is relatively low in small beech trees (around 0.2 for a
387 16m high beech tree based on Bonnesoeur et al. (2013)). The balance between the windthrow and stem
388 breakage risk is among other parameters (rooting depth, soil properties etc.) species and size dependent.
389 Beech is a rather well rooted species with a tendency to break rather than uproot in young stages
390 compared for example to spruce (Stokes, 2000) whereas on very thin soils of Lorraine plateau, beech
391 was described as sensitive species to windthrow with increasing size (Bonnesoeur et al. 2013). This
392 change in mechanical weak point location and failure modes with tree age and size must be considered
393 when studying changes in biomass allocation between compartments. For example Urban (1994)
394 reports a 3 to 9 years delay of the growth response in the stem compared to roots reacting immediately
395 after a road clearing in a 120years old white spruce stand where uprooting might be the main
396 mechanical threat while in younger stands with smaller trees, such delay is in general not observed
397 (Defosse et al., 2022; Nicoll et al., 2019). Higher sensitivity to wind signals of roots when compared
398 to stem was also reported on rather big trees (46 years old spruce (Nicoll and Dunn, 2000)) indicating
399 that the tree size may play an important role in the reactivity of different tree compartments to wind
400 loading.

401 *4.3. Guying changes the pattern of biomass allocation in the tree stem: use of DBH as a proxy to*
402 *predict the root-soil mechanical properties might be risky*

403 Preferential strengthening of the stem does not explain the apparent absence of guying effect on the
404 mechanical properties of the root-soil plate that can be explained differently for thinned trees and for

405 unthinned trees. Unthinned guyed trees exhibited very little growth so that it is difficult to detect any
406 change in the mechanical properties compared to unthinned free trees considering the short treatment
407 duration (4years compared to 30years of growth in same condition). In thinned and guyed trees, the
408 root-soil mechanical properties are not significantly different from uTF trees while its stem biomass
409 increased (Table 1) and that is why the relationship between the root-soil mechanical properties and its
410 empirical predictor has changed. This effect is not the same for the stem resistance that scales with the
411 DBH^3 and as you can see in Figure 7, both predictors do not react in the same way to guying. It
412 indicates that using proxies to predict the root-soil plate performances (or DBH to predict the stem
413 biomass) may be biased if allocation patterns are modified due to environmental stresses. In the next
414 section, we will look at what happens in the structural roots to better understand the guying effect on
415 the biomass allocation inside the tree.



416
417 Fig. 7: Relationship between the stem biomass and the diameter at breast height elevated at power three for different
418 treatments. Dark blue lines and points represent unthinned trees. Light blue lines and points represent thinned trees.
419 Triangles stand for guyed trees and circles for trees free to sway. Solid lines represent regression line for trees free to sway
420 and dotted lines represent regression lines for guyed trees.

421 *4.4. Guying restricts the biomass allocation to mechanically stimulated tree parts while higher*
422 *mechanical loading due to thinning is boosting the stem growth at the expense of structural roots*
423 *reinforcement in line with the mechanical weak point location*

424 The Vent-Eclair experiment designed with the two treatments “thinning” and “guying” aims at
425 studying how the thigmomorphogenetic syndrome is used to control and restore the mechanical
426 stability during the tree life, in natural conditions of disturbance of both resource availability and
427 mechanical stimulation. In this paper, we focus on anchorage stability. As mechanical properties of the
428 root-soil plate integrates 30years of the growth in the same condition and only 4 years under different
429 treatments, the effect of thinning and guying is not easy to track. We therefore looked not only on
430 global properties (stem biomass, root-soil plate mechanical behaviour) but also on growth and on the
431 growth allocation between different tree compartments during the four years before and after the
432 treatment to analyse changes in the biomass allocation. Figure 5b shows that in thinned trees free to
433 sway the biomass is preferentially allocated to the stem instead of roots, pattern that is not observed in

434 thinned and guyed trees. Further, growth of both structural roots and the lower part of the stem is highly
435 reduced in unthinned and guyed trees. In our dataset, effect of thinning and guying was lower in the
436 first year, which was the driest one, for both tree compartments with no delay between the root and the
437 stem growth response (not shown). These results support the idea of a reinforcement of mechanically
438 most stimulated and so risky points and suggest that further developments should investigate how it is
439 physiologically driven (how can growing cells be coordinated inside the whole tree to prioritize the
440 weakest point) and how the priorities are enhanced in case of poor light or water resources. Comparing
441 species and developmental stages of very different patterns of weakness and weakest compartments
442 should be useful to develop a consistent theory, including also the different ways of filtering wind
443 forces through the tree aerial architecture. Such a global view should provide help to go further the
444 current studies focused on a very limited range of species, ages and conditions. For instance, we might
445 expect great differences between conifers (mainly studied up to now) and angiosperms.

446

447 **5. Conclusion**

448 In this paper, we examined the growth and mechanical properties of different tree compartments (stem
449 and root/root-soil plate) in forty beech poles in representative naturally regenerated managed forests of
450 North Eastern France, with high stem density. We submitted trees to a factorial experiment with (i)
451 thinning that stimulated growth and enhanced wind risk and mechanical stimuli, and (ii) guying to
452 remove mechanical stimuli in stems and roots. After four years, we made field mechanical tests to
453 quantify the root soil plate strength and stiffness, and we measured growth in different compartments.
454 We believe that such an experiment (natural or silvicultural disturbance x guying) should be usefully
455 replicated in many situations (species, developmental stages, silvicultures) with improvements in root
456 volume and growth measurements. Measurements of wood mechanical properties in stem and roots as
457 well as other tree traits as crown architecture and hydraulic conductivity and safety should be added.
458 Such a network and database of thinning x guying experiments should support the design of a unified
459 theory of the biomechanical control of growth allocation and its role in tree resistance to winds, using
460 disturbance situations (thinning or other natural gap opening) to manipulate both growth and risk.
461 Results would be included in new generations of process-based forest growth models, avoiding ad hoc
462 laws for allocating growth between the different compartments. As this paper suggests a priority to the
463 weakest point (here the stem, but probably the anchorage in other situations), such a network of
464 experiments representing a range of weakest points (stem breaks or anchorage failure) will provide a
465 clear answer about how priorities of allocation between the different compartments are controlled by
466 mechanical risk and stimuli and/or by other factors as hydraulic functioning or soil constraints to root
467 development. Generally speaking, it supports new visions of growth allocation in respect to forest
468 resistance and resilience, connecting ecological and silvicultural approaches to physiological
469 knowledge on the response of growth processes from living cells to signalling (mechanical signals or
470 others in interaction).

471

472 **CRedit authorship contribution statement**

473 **Jana Dlouha:** Methodology, Data collection, Data analysis, Writing – original draft, Writing-review
474 & editing. **Pauline Défossez:** Methodology, Data analysis. **Joel HDK Jiazet:** Data collection, Data
475 analysis. **François Ningre:** Tree selection, Data collection, Writing – review & editing. **Meriem**

476 **Fournier:** Conceptualisation, Methodology, Writing - review & editing. **Thierry Constant:**
477 Conceptualisation, Methodology, Data collection, Data analysis, Writing – review & editing.

478 **Declaration of Competing Interest**

479 The authors declare that they have no known competing financial interests or personal relationships
480 that could have appeared to influence the work reported in this paper.

481 **Data availability**

482 Data will be made available on request.

483 **Acknowledgements**

484 Authors sincerely thank all members of SilvaTech plateforme and Sylviculture Pole of SILVA
485 laboratory, INRAE Grand-Est for the technical help on the field and during the stem and root samples
486 characterisation. This work was funded as part of a PhD project by supported by “Région Grand Est”
487 and the INRAE division ECODIV. This work was also supported by a grant overseen by the French
488 National Research Agency (ANR) as part of the "Investissements d’Avenir" program (ANR-11-
489 LABX-0002–01, Lab of Excellence ARBRE).

490

491

492

- 494 Achim, A., Ruel, J.C., Gardiner, B.A., 2005a. Evaluating the effect of precommercial thinning on the
495 resistance of balsam fir to windthrow through experimentation, modelling, and development of
496 simple indices. *Can. J. For. Res.* 35, 1844–1853. <https://doi.org/10.1139/x05-130>
- 497 Achim, A., Ruel, J.C., Gardiner, B.A., Laflamme, G., Meunier, S., 2005b. Modelling the
498 vulnerability of balsam fir forests to wind damage. *For. Ecol. Manage.* 204, 35–50.
499 <https://doi.org/10.1016/j.foreco.2004.07.072>
- 500 Albrecht, A., Hanewinkel, M., Bauhus, J., Kohnle, U., 2012. How does silviculture affect storm
501 damage in forests of south-western Germany? Results from empirical modeling based on long-
502 term observations. *Eur. J. For. Res.* 131, 229–247. <https://doi.org/10.1007/s10342-010-0432-x>
- 503 Albrecht, A.T., Fortin, M., Kohnle, U., Ningre, F., 2015. Coupling a tree growth model with storm
504 damage modeling – Conceptual approach and results of scenario simulations. *Environ. Model.*
505 *Softw.* 69, 63–76. <https://doi.org/https://doi.org/10.1016/j.envsoft.2015.03.004>
- 506 Bonnesoeur, V., Constant, T., Moulia, B., Fournier, M., 2016. Forest trees filter chronic wind-signals
507 to acclimate to high winds. *New Phytol.* 210, 850–860. <https://doi.org/10.1111/nph.13836>
- 508 Bonnesoeur, V., Fournier, M., Bock, J., Badeau, V., Fortin, M., Colin, F., 2013. Improving statistical
509 windthrow modeling of 2 *Fagus sylvatica* stand structures through mechanical analysis. *For.*
510 *Ecol. Manage.* 289, 535–543. <https://doi.org/10.1016/j.foreco.2012.10.001>
- 511 Brudi, E., Wassenaer, P., 2001. Trees and statics: nondestructive failure analysis., in: Thomas ES,
512 K.D. (Ed.), *Tree Structure and Mechanics Conference Proceedings: How Trees Stand up and*
513 *Fall down.* International Soc. of Arboriculture. pp. 53–69.
- 514 Constant, T., Bonnesoeur, V., Chaumet, M., Ningre, F., Farré, E., Fournier, M., Moulia, B., 2018.
515 Disentangling the effects of mechanical stimulations in the tree growth response after thinning:
516 First results of an experiment carried out in a beech stand, in: 9th International Plant
517 Biomechanics Conference, August 9-14. Montreal, Canada.
- 518 Coutts, M.P., 1986. Components of Tree Stability in Sitka Spruce on Peaty Gley Soil. *For. An Int. J.*
519 *For. Res.* 59, 173–197. <https://doi.org/10.1093/forestry/59.2.173>
- 520 Coutts, M.P., Nielsen, C.C.N., Nicoll, B.C., 2000. The development of symmetry, rigidity and
521 anchorage in the structural root system of conifers, in: Stokes, A. (Ed.), *The Supporting Roots of*
522 *Trees and Woody Plants: Form, Function and Physiology.* Springer Netherlands, Dordrecht, pp.
523 3–17. https://doi.org/10.1007/978-94-017-3469-1_1
- 524 Cremer, K.W., Borough, C.J., McKinell, F.H., Carter, P.R., 1982. Effects of staking and thinning on
525 wind damage in plantations. *New Zeal. J. For. Sci.* 12, 244–268.
- 526 Cucchi, V., Meredieu, C., Stokes, A., Berthier, S., Bert, D., Najar, M., Denis, A., Lastennet, R., 2004.
527 Root anchorage of inner and edge trees in stands of Maritime pine (*Pinus pinaster* Ait.) growing
528 in different podzolic soil conditions. *Trees* 18, 460–466. <https://doi.org/10.1007/s00468-004-0330-2>
- 530 Defosse, P., Rajaonalison, F., Bosc, A., 2022. How wind acclimation impacts *Pinus pinaster* growth
531 in comparison to resource availability. *FORESTRY* 95, 118–129.
532 <https://doi.org/10.1093/forestry/cpab028>
- 533 Detter, A., Rust, S., Krišāns, O., 2023. Experimental Test of Non-Destructive Methods to Assess the
534 Anchorage of Trees. *Forests* 14. <https://doi.org/10.3390/f14030533>

- 535 Dlouhá, J., Ruelle, J., Constant, T., Ningre, F., Fournier, M., 2023. Beech poles do not produce
536 flexure wood after mechanical stimulation: how size and allometry changes the strategy to resist
537 the wind load. Prep.
- 538 Dongmo Keumo Jiazet, J.H., 2022. Acclimation of trees to increased wind loads following thinning
539 in a Beech stand. AgroParisTech.
- 540 Dongmo Keumo Jiazet, J.H., Dlouha, J., Fournier, M., Moulia, B., Ningre, F., Constant, T., 2022. No
541 matter how much space and light are available, radial growth distribution in *Fagus sylvatica* L.
542 trees is under strong biomechanical control. *Ann. For. Sci.* 79. [https://doi.org/10.1186/s13595-](https://doi.org/10.1186/s13595-022-01162-8)
543 [022-01162-8](https://doi.org/10.1186/s13595-022-01162-8)
- 544 Dupuy, L.X., Fourcaud, T., Lac, P., Stokes, A., 2007. A generic 3d finite element model of tree
545 anchorage integrating soil mechanics and real root system architecture. *Am. J. Bot.* 94, 1506–
546 1514. <https://doi.org/10.3732/ajb.94.9.1506>
- 547 Gardiner, B., Byrne, K., Hale, S., Kamimura, K., Mitchell, S.J., Peltola, H., Ruel, J.-C., 2008. A
548 review of mechanistic modelling of wind damage risk to forests. *Forestry* 81, 447–463.
549 <https://doi.org/10.1093/forestry/cpn022>
- 550 Gardiner, B., Peltola, H., Kellomaki, S., 2000. Comparison of two models for predicting the critical
551 wind speeds required to damage coniferous trees. *Ecol. Modell.* 129, 1–23.
552 [https://doi.org/10.1016/S0304-3800\(00\)00220-9](https://doi.org/10.1016/S0304-3800(00)00220-9)
- 553 Hale, S.E., Gardiner, B.A., Wellpott, A., Nicoll, B.C., Achim, A., 2012. Wind loading of trees:
554 influence of tree size and competition. *Eur. J. For. Res.* 131, 203–217.
555 <https://doi.org/10.1007/s10342-010-0448-2>
- 556 James, K., Hallam, C., Spencer, C., 2013. Tree stability in winds: Measurements of root plate tilt.
557 *Biosyst. Eng.* 115, 324–331. [https://doi.org/https://doi.org/10.1016/j.biosystemseng.2013.02.010](https://doi.org/10.1016/j.biosystemseng.2013.02.010)
- 558 Jonsson, M.J., Foetzki, A., Kalberer, M., Lundstroem, T., Ammann, W., Stoeckli, V., 2006. Root-soil
559 rotation stiffness of Norway spruce (*Picea abies* (L.) Karst) growing on subalpine forested
560 slopes. *Plant Soil* 285, 267–277. <https://doi.org/10.1007/s11104-006-9013-7>
- 561 Kamimura, K., Gardiner, B.A., Koga, S., 2017. Observations and predictions of wind damage to
562 *Larix kaempferi* trees following thinning at an early growth stage. *FORESTRY* 90, 530–540.
563 <https://doi.org/10.1093/forestry/cpx006>
- 564 Kneeshaw, D., Williams, H., Nikinmaa, E., Messier, C., 2002. Patterns of above- and below-ground
565 response of understory conifer release 6 years after partial cutting. *Can. J. For. Res.* 32, 255–
566 265. <https://doi.org/10.1139/X01-190>
- 567 López, B.C., Sabate, S., Gracia, C.A., 2003. Thinning effects on carbon allocation to fine roots in a
568 *Quercus ilex* forest. *Tree Physiol.* 23, 1217–1224. <https://doi.org/10.1093/treephys/23.17.1217>
- 569 Lundstrom, T., Jonsson, M.J., Kalberer, M., 2007. The root-soil system of Norway spruce subjected
570 to turning moment: resistance as a function of rotation. *Plant Soil* 300, 35–49.
571 <https://doi.org/10.1007/s11104-007-9386-2>
- 572 Mitchell, S.J., 2000. Stem growth responses in Douglas-fir and Sitka spruce following thinning:
573 implications for assessing wind-firmness. *For. Ecol. Manage.* 135, 105–114.
574 [https://doi.org/http://dx.doi.org/10.1016/S0378-1127\(00\)00302-9](https://doi.org/http://dx.doi.org/10.1016/S0378-1127(00)00302-9)
- 575 Moulia, B., Coutand, C., Julien, J.-L., 2015. Mechanosensitive control of plant growth: bearing the
576 load, sensing, transducing, and responding. *Front. Plant Sci.* 6, 52.

- 577 Nicoll, B., Achim, A., Crossley, A., Gardiner, B., Mochan, S., 2009. The effects of spacing on root
578 anchorage and tree stability. *Scottish For.* 63, 32–36.
- 579 Nicoll, B.C., Connolly, T., Gardiner, B.A., 2019. Changes in Spruce Growth and Biomass Allocation
580 Following Thinning and Guying Treatments. *Forests* 10, 253.
- 581 Nicoll, B.C., Dunn, A.J., 2000. The effects of wind speed and direction on radial growth of structural
582 roots, in: Stokes, A. (Ed.), *The Supporting Roots of Trees and Woody Plants: Form, Function*
583 *and Physiology*. Springer Netherlands, Dordrecht, pp. 219–225. [https://doi.org/10.1007/978-94-](https://doi.org/10.1007/978-94-017-3469-1_21)
584 [017-3469-1_21](https://doi.org/10.1007/978-94-017-3469-1_21)
- 585 Nicoll, B.C., Gardiner, B.A., Peace, A.J., 2008. Improvements in anchorage provided by the
586 acclimation of forest trees to wind stress. *FORESTRY* 81, 389–398.
587 <https://doi.org/10.1093/forestry/cpn021>
- 588 Nicoll, B.C., Gardiner, B.A., Rayner, B., Peace, A.J., 2006. Anchorage of coniferous trees in relation
589 to species, soil type, and rooting depth. *Can. J. For. Res. Can. Rech. For.* 36, 1871–1883.
590 <https://doi.org/10.1139/X06-072>
- 591 Nicoll, B.C., Ray, D., 1996. Adaptive growth of tree root systems in response to wind action and site
592 conditions. *TREE Physiol.* 16, 891–898.
- 593 Pang, Y., Tian, J., Yang, H., Zhang, K., Wang, D., 2022. Responses of Fine Roots at Different Soil
594 Depths to Different Thinning Intensities in a Secondary Forest in the Qinling Mountains, China.
595 *BIOLOGY-BASEL* 11. <https://doi.org/10.3390/biology11030351>
- 596 Peltola, H.M., 2006. Mechanical stability of trees under static loads. *Am. J. Bot.* 93, 1501–1511.
597 <https://doi.org/10.3732/ajb.93.10.1501>
- 598 R Core Team, 2020. *R: A Language and Environment for Statistical Computing*.
599 <https://doi.org/10.1038/sj.hdy.6800737>
- 600 Rudnicki, M., Meyer, T.H., Lieffers, V.J., Silins, U., Webb, V.A., 2008. The periodic motion of
601 lodgepole pine trees as affected by collisions with neighbors. *Trees* 22, 475–482.
602 <https://doi.org/10.1007/s00468-007-0207-2>
- 603 Ruel, J.C., Larouche, C., Achim, A., 2003. Changes in root morphology after precommercial thinning
604 in balsam fir stands. *Can. J. For. Res. Can. Rech. For.* 33, 2452–2459.
605 <https://doi.org/10.1139/X03-178>
- 606 Stokes, A., 2000. *The supporting roots of trees and woody plants: form, function and physiology*.
607 Kluwer Academic Publishers, Dordrecht, Netherlands.
- 608 Telewski, F.W., 2006. A unified hypothesis of mechanoperception in plants. *Am. J. Bot.* 93, 1466–
609 1476. <https://doi.org/10.3732/ajb.93.10.1466>
- 610 Urban, S.T., Lieffers, V.J., Macdonald, S.E., 1994. Release in radial growth in the trunk and
611 structural roots of white spruce as measured by dendrochronology. *Can. J. For. Res. Can. Rech.*
612 *For.* 24, 1550–1556. <https://doi.org/10.1139/x94-202>
- 613 Valinger, E., Fridman, J., 2011. Factors affecting the probability of windthrow at stand level as a
614 result of Gudrun winter storm in southern Sweden. *For. Ecol. Manage.* 262, 398–403.
615 <https://doi.org/10.1016/j.foreco.2011.04.004>
- 616 Vincent, M., Krause, C., Zhang, S.Y., 2009. Radial growth response of black spruce roots and stems
617 to commercial thinning in the boreal forest. *FORESTRY* 82, 557–571.

- 618 <https://doi.org/10.1093/forestry/cpp025>
- 619 Wallentin, C., Nilsson, U., 2014. Storm and snow damage in a Norway spruce thinning experiment in
620 southern Sweden. *FORESTRY* 87, 229–238. <https://doi.org/10.1093/forestry/cpt046>
- 621 Webb, V.A., Rudnicki, M., Muppa, S.K., 2013. Analysis of tree sway and crown collisions for
622 managed *Pinus resinosa* in southern Maine. *For. Ecol. Manage.* 302, 193–199.
623 <https://doi.org/10.1016/j.foreco.2013.02.033>
- 624 Yang, M., Defossez, P., Danjon, F., Fourcaud, T., 2018. Analyzing key factors of roots and soil
625 contributing to tree anchorage of *Pinus* species. *TREES-STRUCTURE Funct.* 32, 703–712.
626 <https://doi.org/10.1007/s00468-018-1665-4>
- 627 Yang, M., Defossez, P., Dupont, S., 2020. A root-to-foliage tree dynamic model for gusty winds
628 during windstorm conditions. *Agric. For. Meteorol.* 287.
629 <https://doi.org/10.1016/j.agrformet.2020.107949>
- 630